ANL-6143
Radiation Effects on Materials
(TID-4500, 15th Ed.)
AEC Research and
Development Report

ARGONNE NATIONAL LABORATORY
9700 South Cass Avenue
Argonne, Illinois

IRRADIATION OF AN ALUMINUM ALLOY-CLAD CERAMIC PELLET-FUELED PLATE

by

A. P. Gavin

Reactor Engineering Division

May 1960

Operated by The University of Chicago
under
Contract W-31-109-eng-38

DISCLAIMER

TABLE OF CONTENTS

LIST OF FIGURES

LIST OF TABLES

IRRADIATION OF AN ALUMINUM ALLOY-CLAD CERAMIC PELLET-FUELED PLATE

by
A. P. Gavin

I. SUMMARY

An aluminum-nickel alloy-clad ceramic-fueled plate of the BORAX-IV type has been examined destructively after irradiation to a maximum burn-up of 7,800 Mw days per ton in the Argonne circulation water loop in the MTR. Irradiation was at 600 psig and 465°F, with local boiling in the area of highest neutron flux and a maximum heat flux of 500,000 Btu/(hr)(ft^2).

The specimen performed satisfactorily in spite of several factors which made the irradiation conditions more severe than those which would be expected to exist in a reactor fueled with this type of element.

Due to the temperature rise caused by a 5-mil scale deposit on the highest flux zone, the lead bonding in this zone was molten for at least part of the irradiation time. The only detectable effect of this occurrence was a slight flattening of the plate in this area.

The corrosion rate of the aluminum-nickel cladding on the element was approximately 10 mils per year. This high corrosion rate is attributable in part to the adverse ratio of aluminum surface area to water volume in the loop experiment. Results of recent out-of-pile investigations of the effect of this parameter on the corrosion rate of this alloy indicate that with a ratio of aluminum surface area to water volume which would be anticipated in a reactor fueled with this type of fuel, the corrosion rate would be considerably reduced. The increased surface temperature of the cladding material due to the high heat flux and a heavy oxide film buildup was also a factor which influenced the corrosion rate.

Only slight breakup of the ceramic pellet fuel was experienced and there was no evidence that the degree of cracking was influenced to any appreciable extent by exposure to radiation.

The unsupported vapor space at the end of each fuel channel was collapsed when the loop was pressure tested to 1500 psig prior to startup. In spite of this occurrence no break in the cladding was experienced. It is considered that minor changes in design could be made to overcome this difficulty.

II. INTRODUCTION

An experiment, designated MTR-W10, was designed to determine the effects of high burnup on the cladding and fuel of an aluminum-1% nickel alloy (M-388)-clad ceramic pellet-fueled plate of the type manufactured at Argonne for the BORAX-IV core. Conditions of irradiation were selected to allow local boiling at the high flux end of the plate at a pressure of 600 psig. Since this was the first MTR loop experiment in which boiling was to be allowed, detailed calculations of temperature and burnout heat flux were required. It was calculated that a bulk water temperature of 465°F would allow the local boiling desired and still allow a reasonable factor of safety against burnout at the maximum heat flux anticipated.

This temperature is somewhat higher than that at which the BORAX-IV reactor operated, but, since out-of-pile corrosion tests had demonstrated the ability of the cladding alloy to stand up under higher temperatures, it was desired to obtain information on the in-pile behavior of the alloy at these temperatures.

III. TEST SPECIMENS

The test specimens were manufactured by the Metallurgy Division using the same procedures and materials used in manufacture of the fuel plates for the BORAX-IV reactor. The cladding consisted of sections cut from the same extrusions used in these plates. Figures 1 and 2 are a photograph and a drawing, respectively, of the miniature plates.

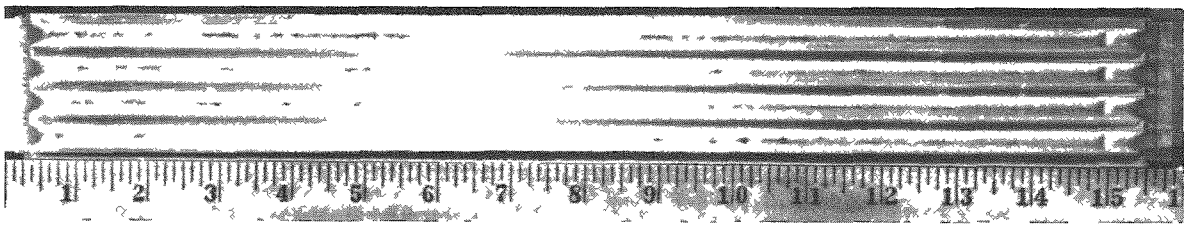

Figure 1
Test Specimen

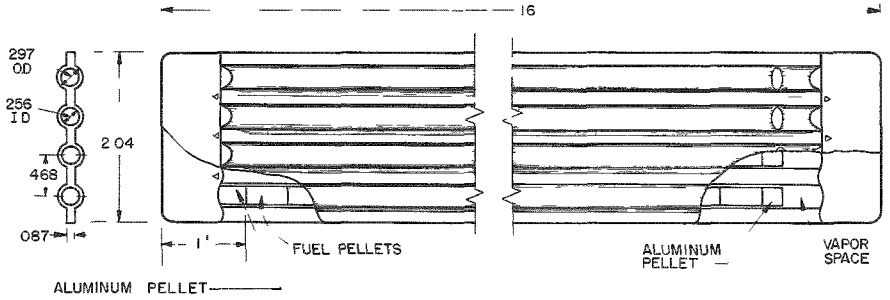

Figure 2
BORAX-IV Prototype Fuel Plate

These elements[1,2] consisted of thoria-urania pellets, bonded with lead in extruded aluminum alloy tube plates. The pellets were $\frac{1}{4}$ in. in diameter and $\frac{1}{2}$ in. long. The pressing mixture for the pellets consisted of 93.4 wt% ThO_2 and 6.54 wt% U_3O_8. The U_3O_8 was 93% enriched. The pellets were fired in air at 1700-1750°F, attaining an average geometric density of 8.3 g/cc and an average apparent density (water immersion) of 9.8 g/cc. The effective cladding thickness was 0.016 in., while the effective thickness of the lead bond was 0.018 in.

The cladding material was M-388 aluminum alloy, which consists of 2S aluminum with 1% nickel added.

Original heat transfer calculations indicated that the desired conditions of pressure and local boiling could not be maintained with safety if the fuel extended beyond one inch from the in-reactor end of the fuel plate. In order to meet this requirement, an aluminum pellet, approximately $\frac{1}{2}$ in. in length, was placed in each fuel channel at the in-reactor end. This is the only way in which the test plates differed from the full-sized plates, either in method of manufacture or materials of construction.

An accurate weight and a complete set of thickness, width, and length measurements were taken on each of the two plates to be used in the experiment before they were loaded into the holding cartridges for the in- and out-of-pile test positions.

IV. IRRADIATION

A. ANL-2 Loop

The test plate was irradiated in the ANL-2 loop in the Materials Testing Reactor at the National Reactor Testing Station in Idaho. This loop is located in a radial beam hole through the graphite reflector of the reactor. The tip of the pressure tube is located near the edge of the reactor core in a cylindrical well in the reactor tank. Due to the radial position of the facility, the flux drops rapidly from the in-reactor end of the fuel section to the outer end.

Loop flow is channeled in through a rectangular tube approximately 1 in. by 2 in. located in the center of the cylindrical pressure tube and out through the space on the outside of the rectangular tube. The fuel element was located at the inner end of the rectangular tube by means of a holding cartridge (see Figures 3 and 4).

Flow through the loop is maintained at the desired rate by circulation pumps, and bulk water temperature is maintained by the use of a temperature controller and electric heaters. Water quality is maintained by means of a bypass ion-exchange system (see Figure 5).

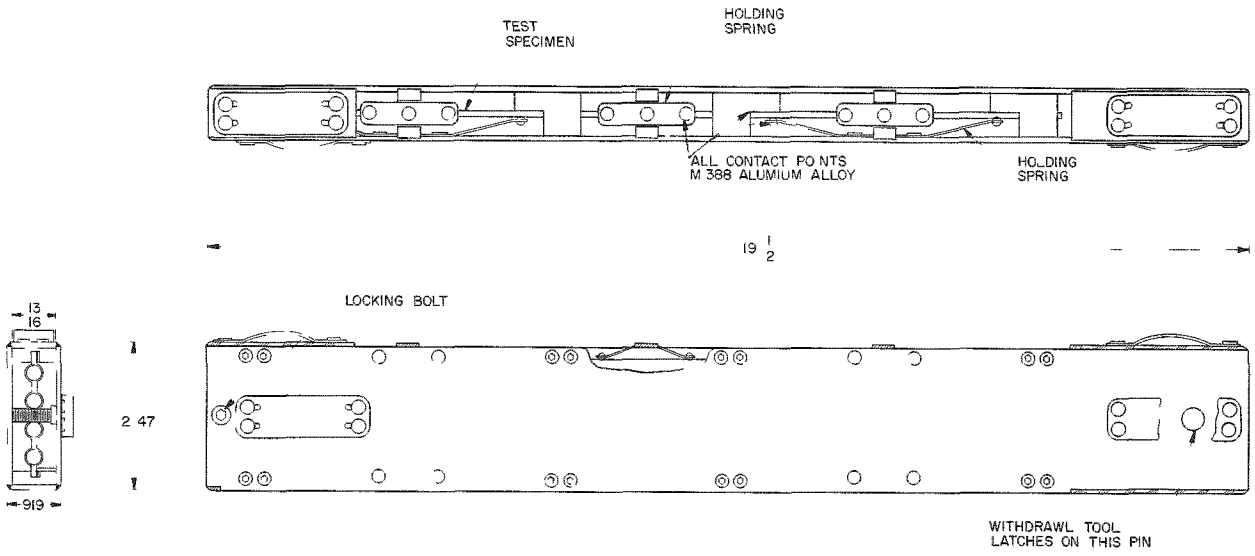

Figure 3
Holding Cartridge - ANL-2 Loop

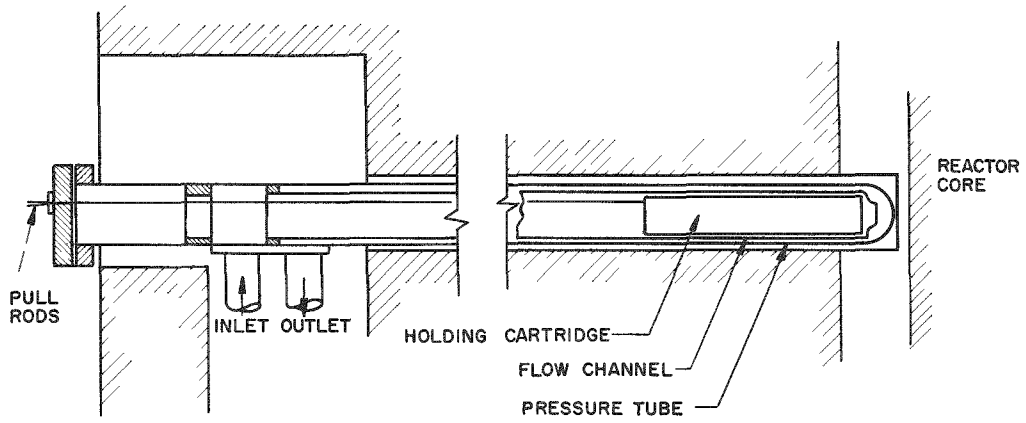

Figure 4
ANL-2 In-Pile Tube

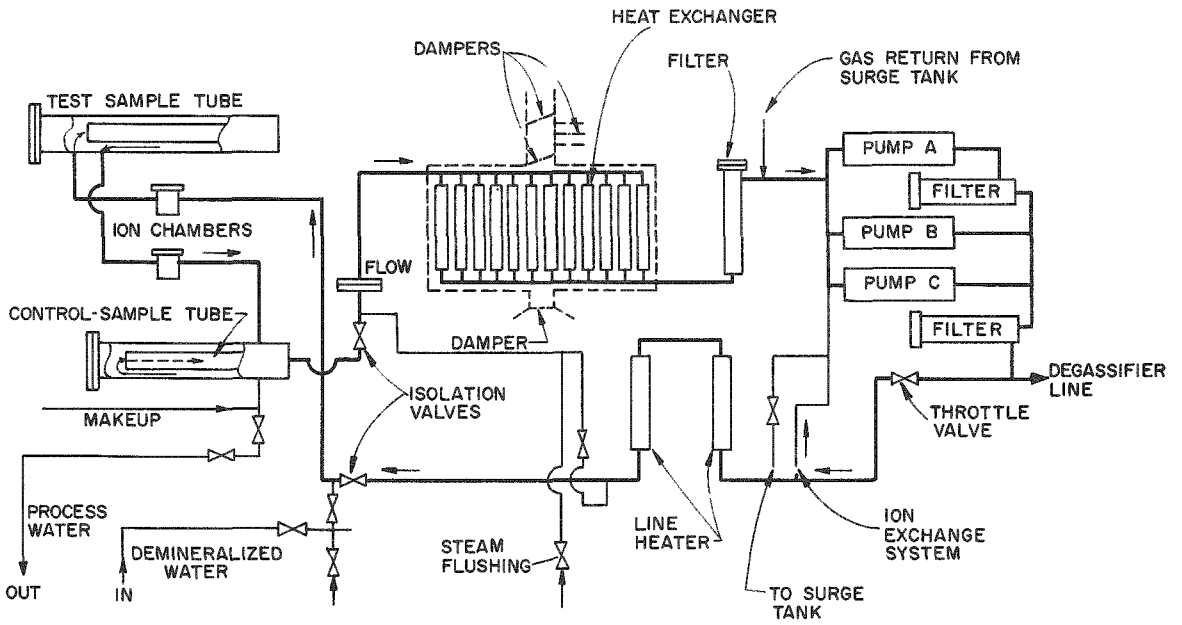

Figure 5
Flow Diagram of Water Loop

To distinguish between the effects of irradiation, and those of exposure to loop water without irradiation a second exposure location is provided in the external portion of the loop.

Reference 7 gives a complete description of the ANL-2 loop.

B. Conditions of Irradiation

In order to determine as closely as possible the flux to which the test plate would be subjected, low-power flux runs were made. One run was made with a set of flux wires fastened to an unfilled fuel plate which was loaded into a holding cartridge and placed in irradiation position in the loop. A second run was made with a similar plate but with scrap fuel pellets in the fuel channels. Both unshielded and cadmium-shielded flux wires were used in each case. These wires were counted for activity at the end of the runs and the resulting flux values extrapolated to full-power conditions by MTR personnel.

Although flux values obtained from these runs were used in making the pre-irradiation calculations for this experiment, a subsequent full-power flux run, one cycle in duration, gave a more reliable flux plot for the loop. The values obtained from this run are somewhat lower than those from the low-power run. Figure 6 is a plot of the thermal flux as

determined by this full-power run. Also included in Figure 6 is a plot of the perturbed flux as calculated using the low values obtained at low power to indicate the amount of perturbance.

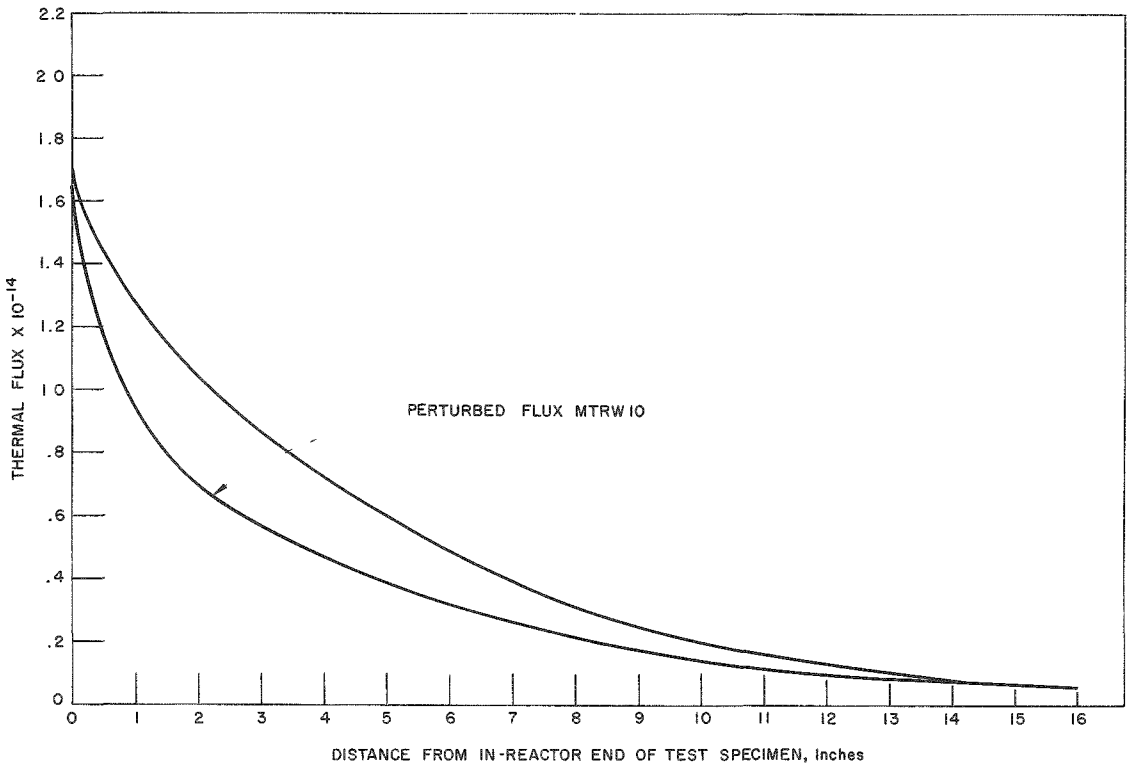

Figure 6
Thermal Neutron Flux Plot ANL-2 Loop In MTR

The fast neutron flux was approximately one-tenth of the slow neutron flux.

Since out-of-pile corrosion data on the M-388 alloy indicated that this material should perform satisfactorily at higher temperatures than those of BORAX-IV, it was decided to run this experiment under conditions which would produce information on the behavior of the cladding alloy under irradiation at these temperatures.(3) With this in mind, the pressure for the experiment was set at 600 psig and calculations were made to determine a temperature at which local boiling would occur on at least a portion of the plate and such that there would be no change of burnout at the maximum heat flux anticipated. The temperature which best fits these requirements was determined to be 465°F.

A complete tabulation of the conditions which existed in the loop during the irradiation is presented in Tables 1 and 2.

Table 1

SUMMARY OF CONDITIONS OF IRRADIATION
MTR-W10

Total Time in Loop	122 Days (MTR Cycles 90-96)
Total Neutron Exposure	2365 Mwd
Temperature (during irradiation	
460-470°F	90.6% of time subject to irradiation
above 440°F	92.7% of time subject to irradiation
Temperature (Total Time in Loop)	See Table 2
Pressure	600 psig
Flow Rate	60 gpm 11-13 feet per second past test specimen
Aluminum Surface Area to Water Volume Ratio	6.4 cm^2/l
Water Resistivity	1.4-3.5 Megohms*
pH	
Average	6.5
Maximum	7.6
Minimum	5.9
Power Fluctuations	
Full-power Cycles (zero power to 40 Mw)	28
Power Dips (40 Mw to $\sim\frac{1}{2}$ power)	9
Dissolved Oxygen	
Less than 0.08 ppm during entire exposure	

* During the first cycle the resistivity varied between 0.2 and 1.4 megohms for a total of approximately 200 hours.

Table 2

TEMPERATURE OF EXPOSURE
FOR W10 FUEL ELEMENT
Total Exposure Time - 122 Days

Temperature of Loop, °F	% of Time above Temperature Indicated	Days above Indicated Temperature
175	100.0	122
200	96.6	118
225	96.0	117
250	95.5	116-1/2
275	94.3	115
300	93.5	114
325	63.7	77-3/4
350	63.7	77-3/4
375	63.3	77-1/4
400	62.1	75-3/4
425	60.6	74
450	58.6	71-1/2
465	55.3	67-1/2

In order to allow for removal of decay heat, a cooling period of one cycle was desired before removal of the element of the loop. Cooling of the element was accomplished by pulling it back out of the flux, using wires which had been attached to the cartridge and which passed out through packing glands in the flange. The cooling period was actually extended to three cycles due to the fact that the reactor operating schedule during this period would not allow the loop to be opened.

Another factor which definitely influenced the results of the irradiation but which could not be directly evaluated was the power fluctuation which occurred in the reactor cycles. For completeness, Table 1 lists those power fluctuations which occurred during the exposure of this element.

Part of the routine of starting up the loop after inserting a new test specimen is to subject the entire assembly to a cold hydrostatic test of 1500 psi. Ordinarily this procedure is of no consequence to the test, but in this case, due to a fault in the design of the test specimen, the vapor spaces on the end of the fuel tubes of the element were collapsed. This is discussed further in Section VI.

V. POSTIRRADIATION EXAMINATION

A. Procedure

1. Appearance and Physical Measurements

The irradiated element was removed from the cartridge and visually examined both through the cave window and under a remote microscope. A complete set of thickness measurements was taken in this "dirty" condition. A similar examination was made on the out-of-pile plate.

2. Removal of Oxide

Oxide was removed from both in-and out-of-pile elements by an electrolytic descaling technique using boric acid as the electrolyte. An alternating current of approximately 0.02 amp/cm^2 was passed through the plate. Samples of the oxide were removed and retained for spectrographic analysis.

3. "Clean" Measurements and Appearance

The plate was then re-examined under the microscope and another set of length, width and thickness measurements were taken.

4. Removal of Cladding

The elements were first cut into four sections by use of a small milling machine equipped with three cutters ganged to sever the webs between the fuel channels. After this separation was completed, the individual channels were coated with microwax and scratched to expose the cladding along each side. These pieces were then immersed in bromine-methanol mixture until the cladding was eaten through sufficiently to allow the two halves of the fuel tube to be separated (see Figure 7).

5. Examination of Fuel

This procedure produced rods of fuel held together by the lead bonding. Each rod was laid on an aluminum plate which was, in turn, placed on an electrically heated hot plate. Heat was applied until all the lead was melted away from the fuel pellets. Before the pellets were completely exposed, it was necessary to remove a thin layer of dark oxide mechanically. The fuel thus exposed was examined visually under the microscope and samples were taken from several positions for burn-up analysis.

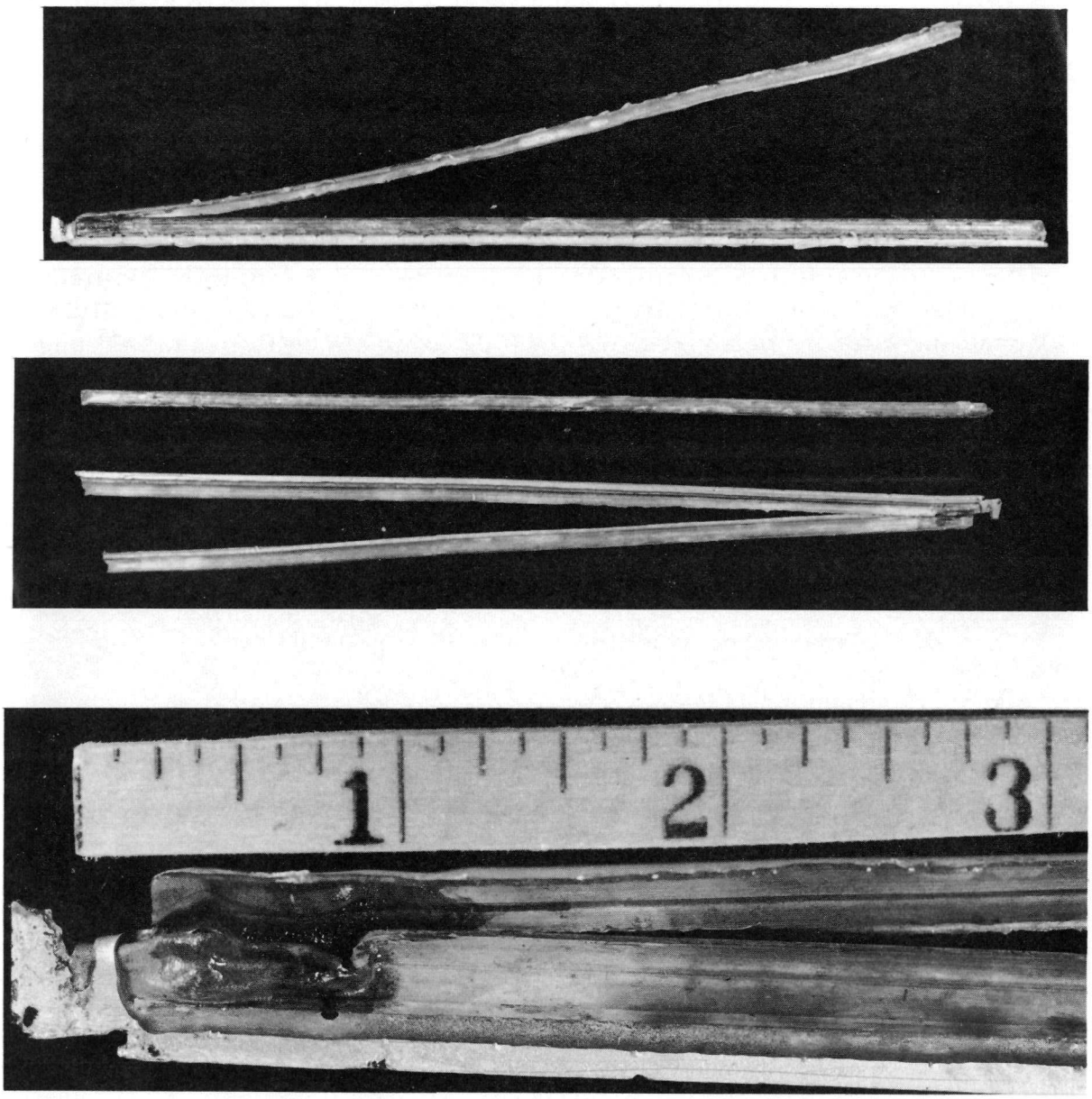

Figure 7
Removal of Cladding

B. Results

1. Appearance

Figure 8 is a photograph of the in-pile plate upon removal from the loop. Figures 8A-8L are photomicrographs of portions of the plate as indicated on Figure 8.

A thin layer of loose red oxide covered the entire width of the fuel plate over an area from approximately one inch to five inches from the in-reactor end. This oxide was easily removed by light brushing with a bristle brush. The remaining oxide was tightly adherent and grey in color. The oxide in the highest flux zone was darker in color than that which covered most of the rest of the plate.

Figure 9 is a photograph of the same plate after removal of the oxide scale. Figures 9A-9G are photomicrographs of portions of the surface of the plate in this condition as indicated on Figure 9. The oxide on the highest flux area was much more adherent than on the remaining portions of the plate. As can be seen from the "clean" photograph, it was found impossible to remove all of the oxide from this area even after repeated applications of the stripping current and considerable "chipping" with a dissecting needle. Scratches caused by the use of this implement are quite evident in some of the photomicrographs and should be discounted when evaluating the effects of the irradiation and exposure. Figure 10 illustrates the appearance of collapsed ends of the fuel channels before and after removal of oxide.

Figure 11 is a composite of one side of the out-of-pile plate before and after descaling. The oxide on this plate was uniform and easily removed by the stripping procedure.

2. Physical Measurements

Table 3 is a summary of the averages of measurements of length, width, and thickness and weight taken before irradiation, as removed from the reactor, and after removal of scale for both in-and out-of-pile plates. A complete tabulation of all measurements taken is included in the Appendix.

Table 4 indicates the loss of cladding thickness and corrosion rate of the aluminum cladding as calculated from the loss in weight. The corrosion calculated in this manner is considerably less than that indicated by the decrease in thickness, but some loss in thickness as measured over the fuel channels due to distortion of the plate during pressure test and irradiation is entirely possible.

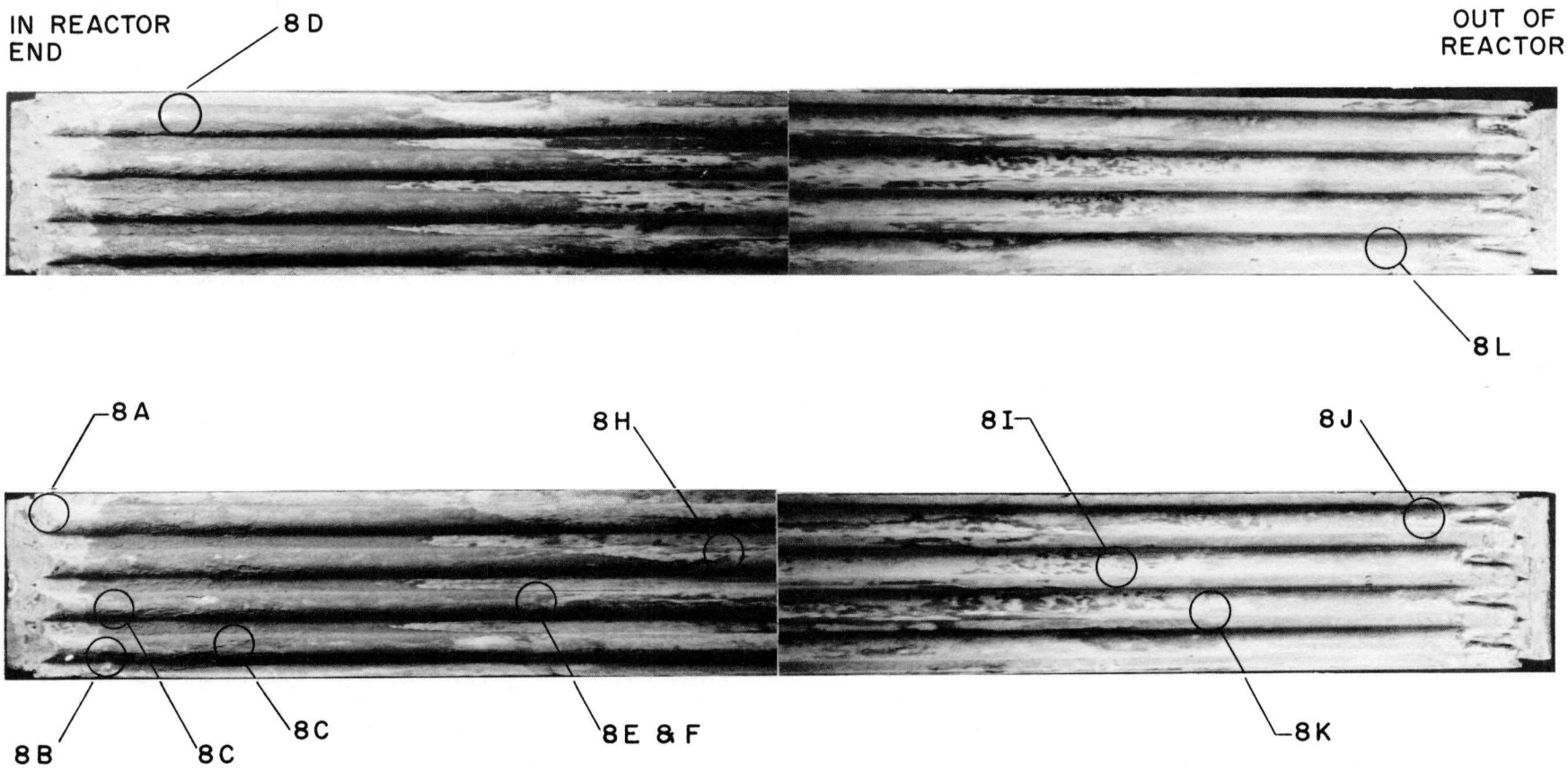

Figure 8

Irradiated Fuel Plate as Removed from Reactor

(3 X) Figure 8A

General Appearance of Aluminum Spacer Pellets. Absence of dark surface oxide.

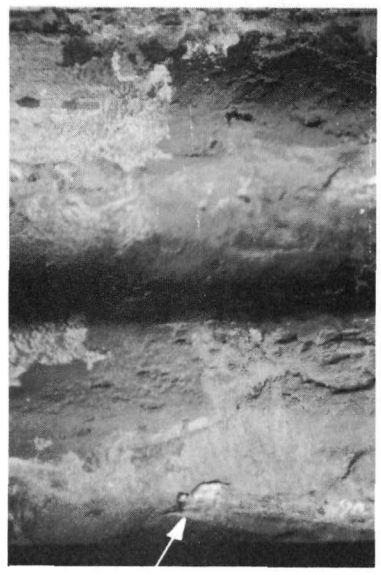

(3 X) Figure 8B

Transition from Aluminum to Fuel Pellets. The presence of the dark surface oxide on the portion of surface where heat flux was highest is evident. Also note slight depression in side of fuel channel indicated by arrow.

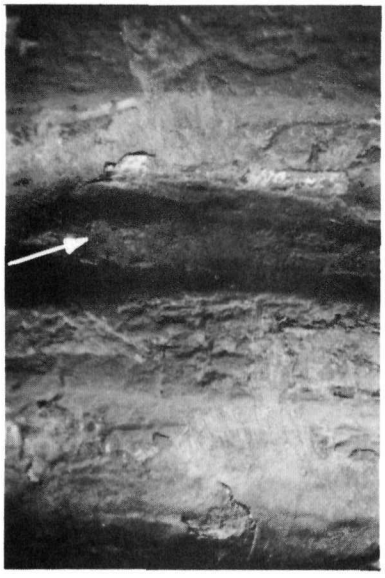

(3.5X) Figure 8C

Depression in Side of Channel. This was the only longitudinal depression noted in fuel portion of plate.

(11 X) Figure 8D

General Appearance - Boiling Surface. Note presence of loose dark oxide on surface and areas where portions of the scale has spalled off.

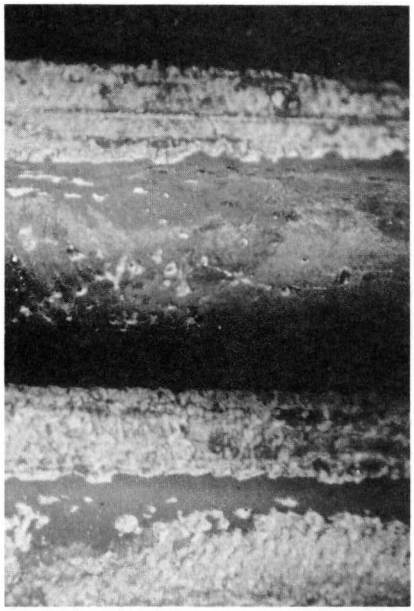

Figure 8E

General Appearance - Outer End of Boiling Area. Note pitting attack which was typical of this area of plate surface.

Figure 8F

Enlargement of 8E. Detail of pits in oxide

Figure 8G

General Appearance of Boiling Area. Rough chipped appearance of oxide typical of surface of portion of plate where boiling occurred.

Figure 8H

General Appearance of Non-Boiling Area. Another more uniform oxide surface typical of non-boiling portions of plate surface.

Figure 8I

Eroded Oxide. Typical of some parts of non-boiling portion of plate surface.

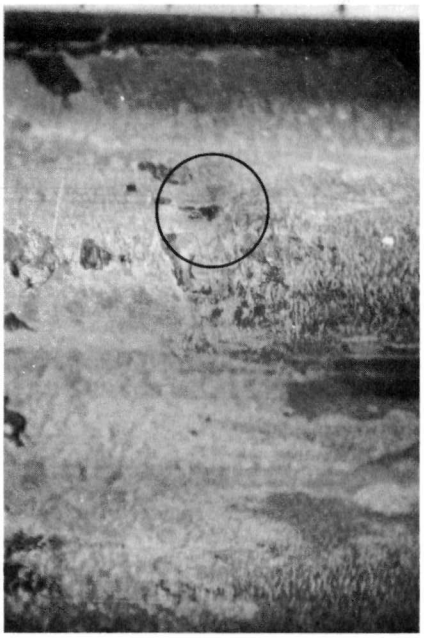

Figure 8J

Slight Depression in Side of Fuel Channel. This is the only defect of this type observed on the cold end of the fuel plate.

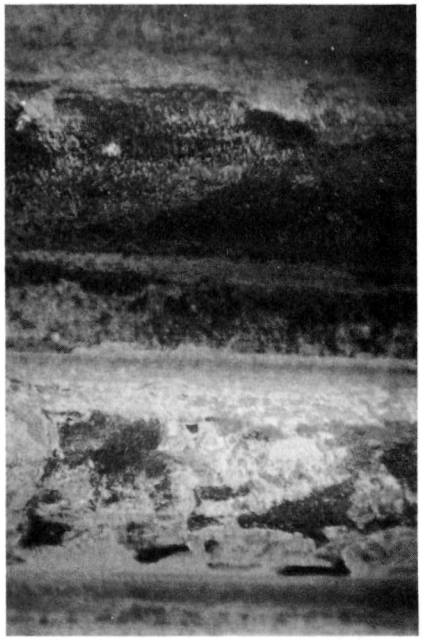

Figure 8K

Typical Appearance of the Outer End of Fuel Plate

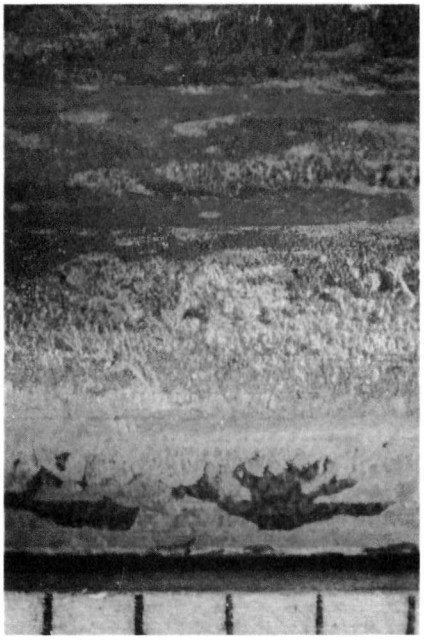

Figure 8L

Enlarged View of Typical Section of Plate Surface on Outer End

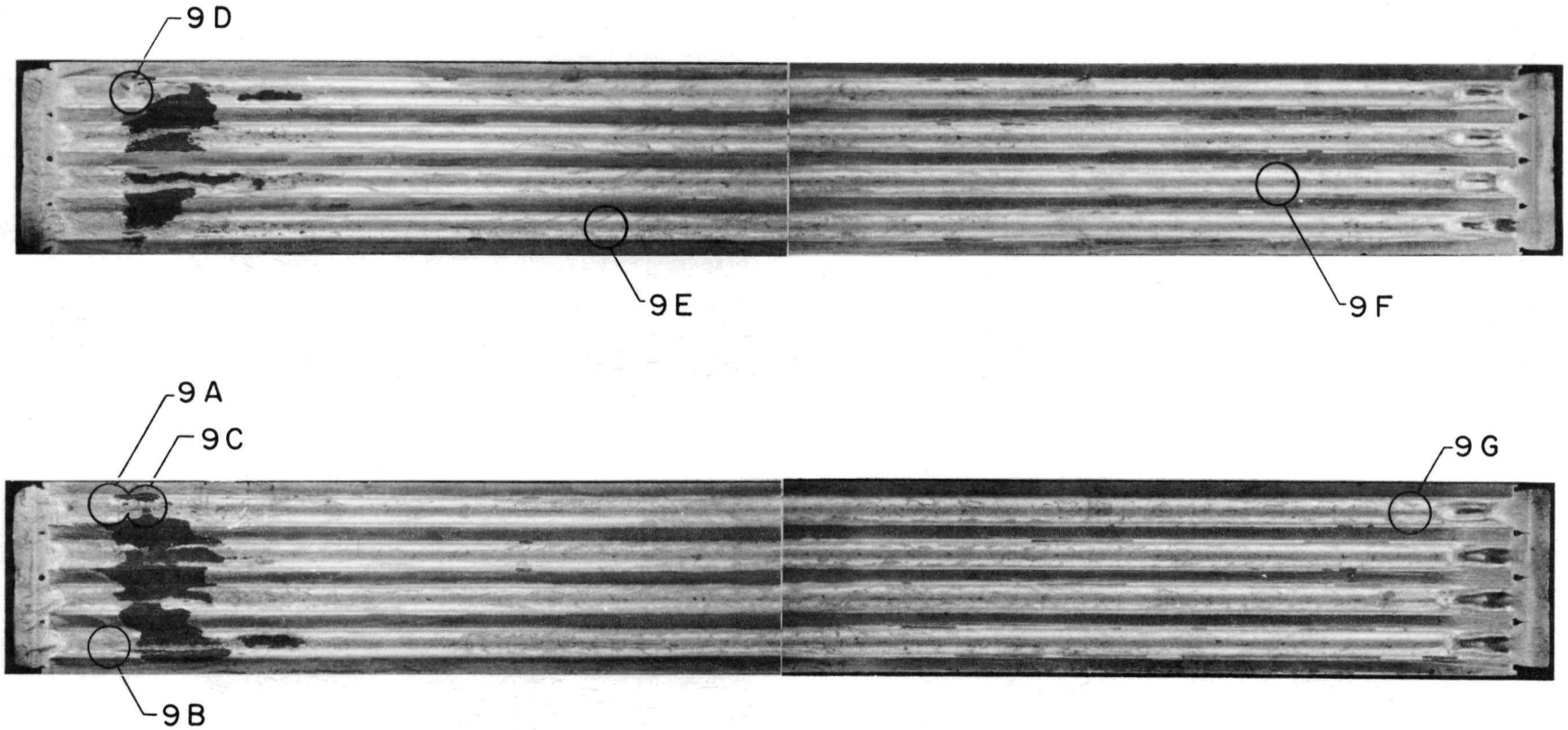

Figure 9

Irradiated Fuel Plate After Removal of Scale

(4-1/2 X) Figure 9A

Transition from Aluminum to Fuel Pellets. Note ridge in aluminum cladding at point where fuel begins. Diameter is smaller over fuel.

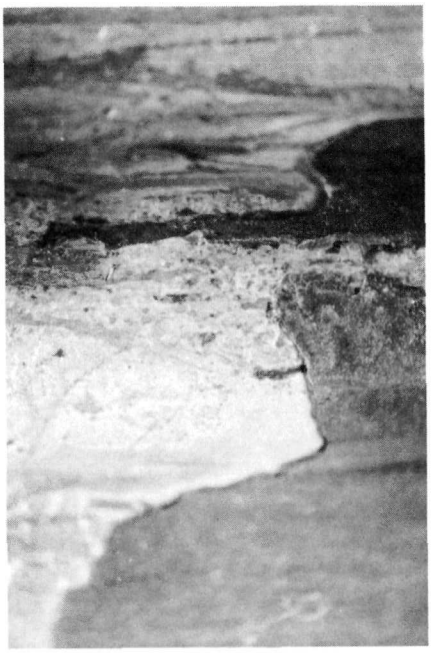

(4-1/2 X) Figure 9B

General Appearance, Area of Highest Burnup. Note very heavy adherent oxide not removed by descaling procedure.

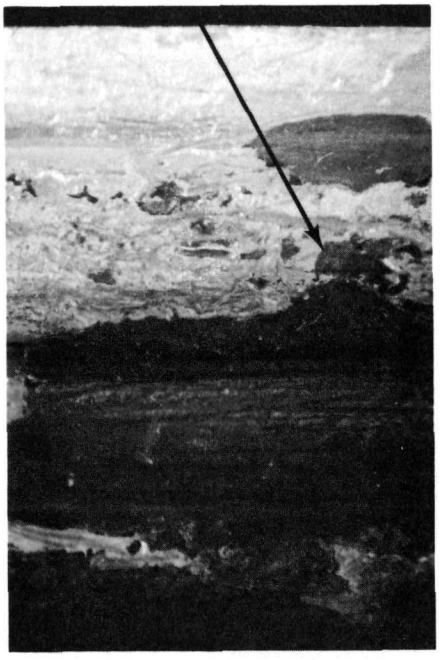

(4-1/2 X)
Figure 9C

Area of Highest Burnup. Indentation indicated is evidently at juncture of two fuel pellets.

(4-1/2 X)
Figure 9D

Edge View of Depression between Aluminum and Fuel Pellets.

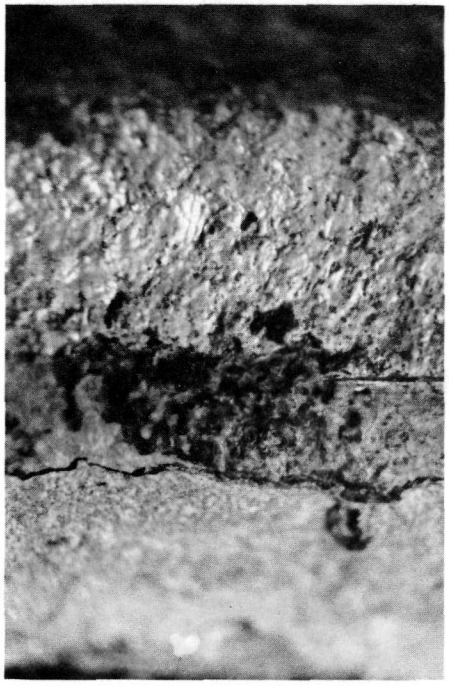

(13X) Figure 9E

General Appearance - Edge of Boiling Zone. Rough appearance is typical of this portion of plate surface and was not noted on either end of the plate.

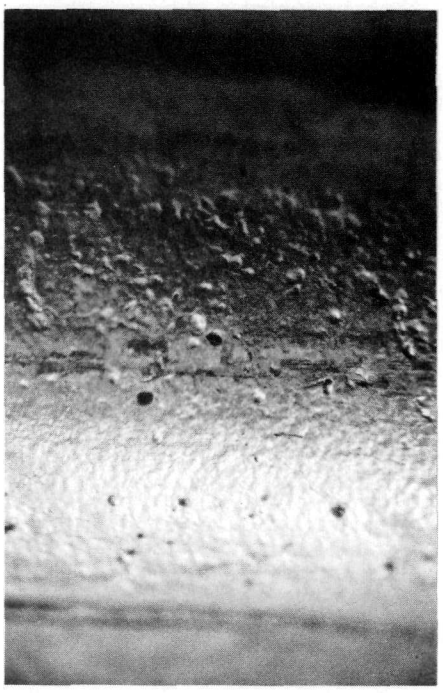

(13X) Figure 9F

Pitting Attack. This type of attack was not general but occurred in only a small area around the location of this photograph.

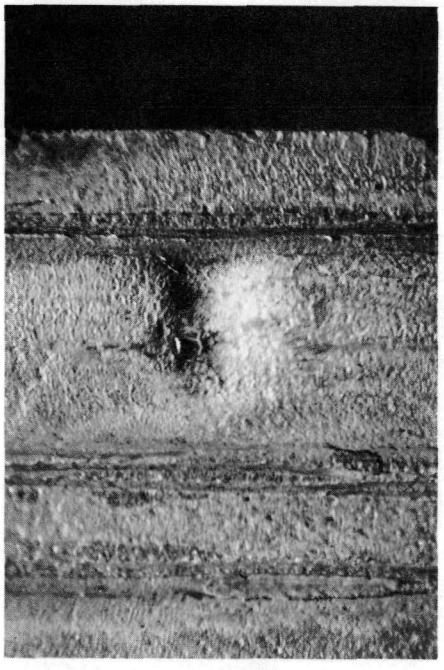

(4X) Figure 9G

Depression Near Outer End of Plate. This is the same flaw illustrated in Figure 8J before descaling.

Number Side

Opposite Side

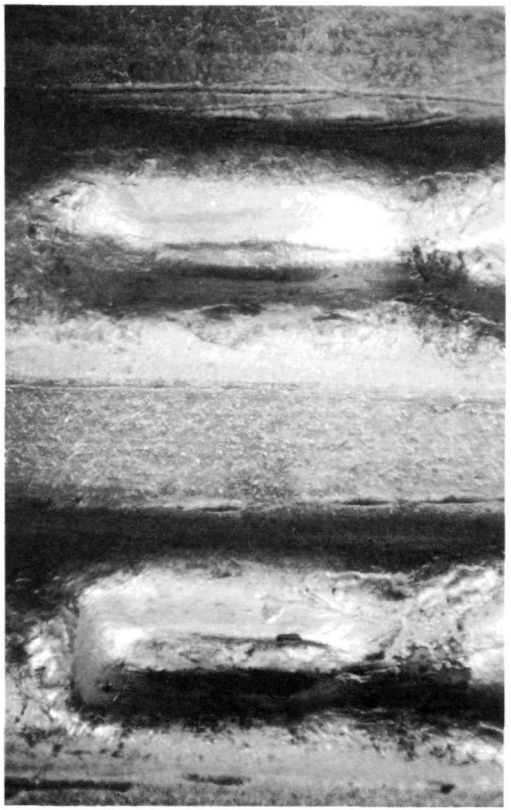

Opposite Side with Scale Removed

Figure 10

Collapsed Ends of Fuel Channels before and after Scale Removal

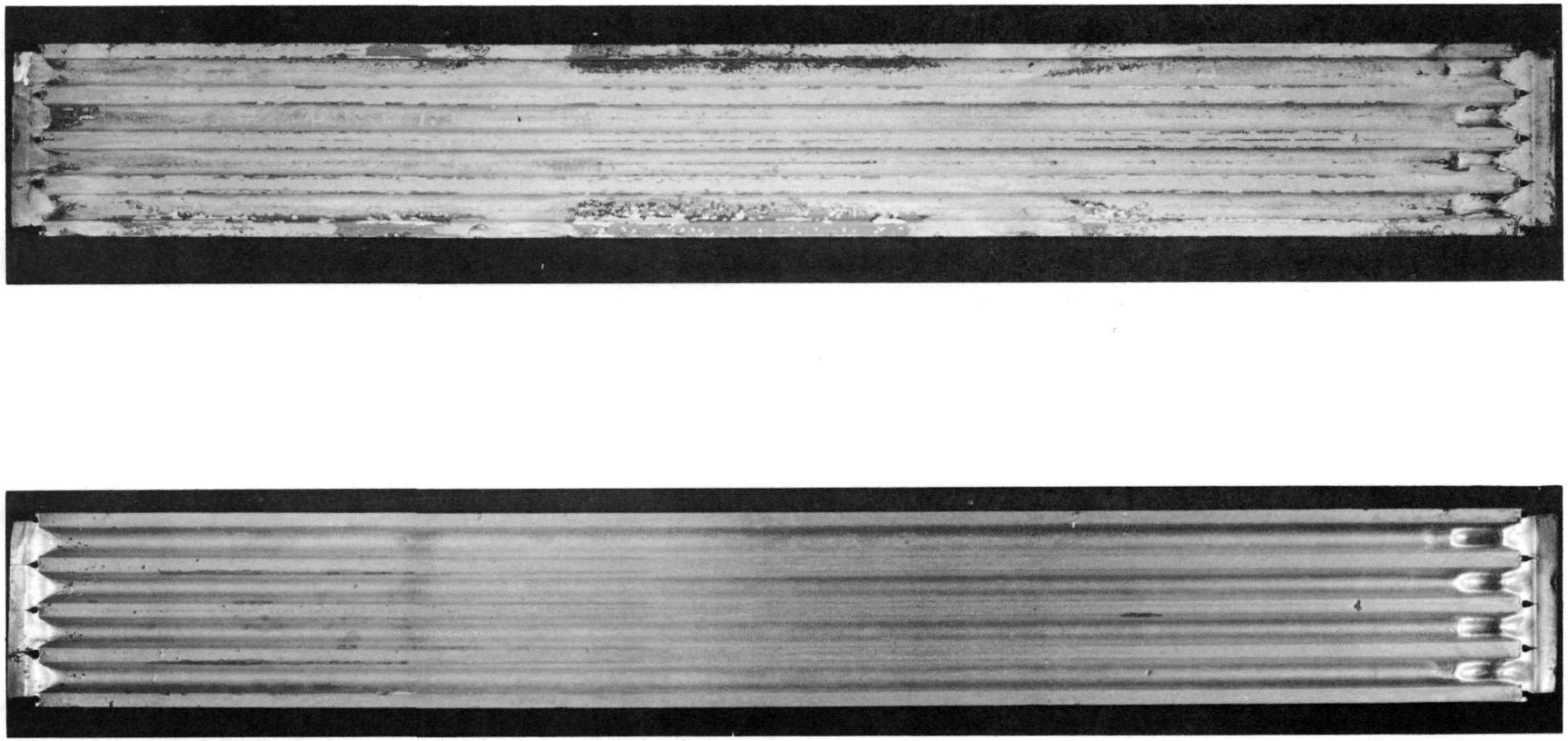

Figure 11

Out-of-Pile Fuel Plate Before and After Removal of Scale

Table 3

SUMMARY OF PHYSICAL DIMENSIONS
W10 In- and Out-of-pile Specimens

Average Dimension	Original	As Removed from Reactor	With Scale Removed
	In-pile Plate		
Thickness (in.)(1)	0.3054	0.3030	0.2997
Width (in.)	2.0040	2.0026	1.999
Length (in.)	16.071	-(2)	-(2)
Weight (g)	541.60	543.62	543.36
	Out-of-pile Plate		
Thickness(1)	0.3012	0.2968	0.2951
Width	2.0006	2.002	1.9950
Length	16.075	16.077	16.080
Weight	511.69	-	507.51

(1) Average thickness measurements exclude collapsed section on both plates and boiling section of in-reactor plate.

(2) The length measurements on the in-pile section are not reliable due to deformation in removing the plate from the holding cartridge.

Table 4

CORROSION RATE
(Based on weight loss)

	In-pile Plate	Out-of-pile Plate
mils (during 122-day exposure)	2.16	1.25
mils/year (based on 74 days above 425°F)	10.6	6.1

Table 5 indicates the thickness of the oxide layer on the in- and out-of-pile plates. These figures were obtained from the difference in thickness before and after removal of the scale.

Table 5

SCALE THICKNESS (mils)

	In-pile Plate	Out-of-pile Plate
Boiling section	5.2	-
Nonboiling section	1.8	1.8

3. Scale Analysis

Table 6 is a summary of data from the spectrochemical analyses of scale from samples taken from various locations on the plate. The "loose red oxide" listed is that which was brushed off of the high-flux area of the plate before the electrolytic descaling operation was begun.

Table 6

SPECTROCHEMICAL ANALYSIS OF OXIDE
(% of metal present)

	Boiling Section 1	Boiling Section 2	Red-Surface Oxide	White Oxide
Al	VS[1](79)	VS(79)	8	VS(97)
Fe	15	17	VS(86)	2
Ni	4	2	4	1
Others	2	2	2	0.5

[1]VS - very strong 100% to 10%

Figure in parentheses is obtained by difference from remainder of analysis.

Analysis of a portion of the scale taken from the boiling portion of the in-pile plate by X-ray diffraction indicated that more than 90% of the material was composed of boehmite (alpha aluminum oxide monohydrate). The remainder was composed of spinel of undetermined composition and corundum (alpha aluminum oxide). Boehmite and a small fraction of corundum were identified in a sample of oxide from the out-of-pile plate.

4. Fuel Pellet Analysis

Table 7 presents the results of burnup analysis of pellets removed from the in-reactor section. Table 8 includes the results of isotopic analysis of the uranium in each fuel specimen. Table 9 is a summary of heat flux and per cent burnup calculated from the analyses presented in Table 7.

Table 7

BURNUP ANALYSIS OF FUEL

Sample Location, inches from In-reactor End	Fissions/g(a)	U atoms/g(b) ($\times 10^{-20}$)
1	$1.9_0 \times 10^{19}$	1.3_4
$1\frac{1}{2}$	$2.3_5 \times 10^{19}$	1.4_4
6	$7.6_3 \times 10^{18}$	1.5_0
8	$8.0_7 \times 10^{18}$	1.4_0
10	$4.0_9 \times 10^{18}$	1.5_1
$13\frac{1}{2}$	$2.1_7 \times 10^{18}$	1.3_0
15	$2.3_3 \times 10^{18}$	1.3_9
Average (integrated)	9.24×10^{18}	

(a) Fissions per gram of sample; calculation is based on U^{235} fission using a 6.1% fission yield, and a half-life of 30.0 years for Cs^{137}.

(b) Uranium atoms per gram of sample; final uranium concentration in sample.

Table 8

ISOTOPIC ANALYSIS OF URANIUM IN IRRADIATED FUEL

Location, Inches from In-reactor End	% by Weight				
	U^{233}	U^{234}	U^{235}	U^{236}	U^{238}
1	8.47 ± 0.08	1.35 ± 0.01	82.86 ± 0.06	0.507 ± 0.005	6.81 ± 0.06
$1\frac{1}{2}$	6.41 ± 0.06	1.19 ± 0.01	81.52 ± 0.12	4.51 ± 0.09	6.37 ± 0.06
6	1.97 ± 0.01	1.02 ± 0.01	89.63 ± 0.05	1.70 ± 0.01	5.68 ± 0.05
8	1.68 ± 0.01	1.01 ± 0.01	90.05 ± 0.05	1.51 ± 0.01	5.75 ± 0.05
10	0.885 ± 0.008	0.99 ± 0.01	91.55 ± 0.05	0.947 ± 0.009	5.63 ± 0.05
$13\frac{1}{2}$	0.502 ± 0.005	0.504 ± 0.005	92.70 ± 0.05	0.744 ± 0.007	5.55 ± 0.05
15	0.485 ± 0.005	0.99 ± 0.01	92.25 ± 0.05	0.646 ± 0.006	5.63 ± 0.05

Table 9

BURNUP AND HEAT FLUX

	Burnup(1) % of Total Metal Atoms	Heat Flux(2) at Fuel Surface, BTU/(ft²)(hr)
Maximum	1.03	497,000
Minimum	0.10	49,300
Average	0.41	195,000
U^{235} content of original pellets: 5.83% of metal core atoms.		

(1) Calculated from burnup analysis.

(2) Average for run - as calculated from burnup analysis.

VI. DISCUSSION OF RESULTS

A. Boiling Area

The appearance of the loose red oxide on the surface of the plate on the area of high heat flux is typical of surfaces which have undergone boiling heat transfer. This would indicate that boiling occurred over an area between the point at which the fuel begins (1 in. from in-reactor end) and approximately five inches back from the in-reactor end of the plate. Calculations based on the heat flux as determined from the burn-up analysis confirm this observation.

B. Collapse of Vapor Spaces

As indicated in Figures 8-11, the fuel channels collapsed completely in the vapor spaces at the end of the element. Subsequent tests and calculations indicate that the unsupported portion of the fuel channels in a plate of this type will collapse in a cold hydrostatic test at pressures between 600 and 1200 psig, thus indicating that the original 1500-psig hydrostatic test of the loop was responsible for the collapse noted.

An autoclave test at 422°F and 300 psig for one week caused partial collapse of the vapor spaces in a duplicate test plate. Indications were that it was only a matter of time before the collapse of the tubes in these unsupported sections would be complete. This makes it apparent that if collapse of the channels of the loop test specimens had not been caused by the initial pressure check, exposure to the pressure and temperature of the loop test would have produced the same end result.

While this collapse of the fuel channels did not cause any break in the cladding in the loop experiment, it was the cause of the ultimate failure of the BORAX-IV core.[4,5]

It is believed that this defect could be overcome by slight changes in the design and manufacturing process of the plates.

C. Corrosion of Cladding Alloy

The corrosion rate of 10.6 mils/yr listed in Table 4 is an average for the entire surface of the in-pile plate as determined by weight loss during the irradiation period. This is somewhat higher than the rate of 6.1 mils/yr determined in the same manner for the out-of-pile plate. Thickness measurements taken on a piece of cladding removed from the hot specimen indicated that the amount of cladding lost on the inner one-third of the plate was roughly twice the average. It is believed that this higher corrosion rate in the high-flux zone is due to the increased surface temperature and not a result of exposure to irradiation.

In a reactor fueled with fuel elements clad with this same alloy and run under conditions of pressure, temperature, and water quality similar to those of this experiment, the cladding material would not be expected to corrode at as high a rate as that determined in this test. The main reason for anticipating a lower corrosion rate in such a reactor is that the ratio of aluminum surface area to water volume would be expected to be very much higher than that which existed in the loop test. This ratio has been demonstrated to have a decided effect on the corrosion rate of M-388 aluminum alloy.[3,9]

D. Scale and Fuel Temperatures

Recent measurements of the thermal conductivity of fuel element scale of approximately the same composition and crystal formation as that found on the boiling section of this plate indicate that the correct value of this factor is between 1.0 and 0.5 Btu/(hr)(ft^2)(°F)/(ft).[8] With the measured 5.2 mils of scale and a heat flux of 500,000 Btu/(hr)(ft^2), these conductivity values indicated that the temperature rise through the oxide layer was between 220 and 425°F. The calculated temperature difference through the surface film at this point is approximately 55°F. Adding these values to the bulk water temperature of 465°F yields a temperature of between 740 and 945°F at the surface of the plate. The melting point of lead is 618°F. Thus, melting of the lead bonding over a portion of the length of the test plate is definitely indicated.

The presence of corundum in the oxide scale also indicates that temperatures in this range were reached. This dehydrated phase of aluminum oxide is formed from the hydrated boehmite only at temperatures above 720°F.[6]

The dimensions of the test plate after irradiation and removal of scale showed a decided decrease in thickness and an increase in width in the region from one to two inches from the in-reactor end of the element. This flattening of the plate is probably also a result of melting of the bonding material.

Another phenomenon which might be partially due to very high temperatures in this region of the plate is the adhesion of the cladding material to the lead bonding. In the out-of-pile plate and in the areas of lower flux of the in-pile plate no difficulty was experienced in separating the cladding material from the lead-covered fuel. In the high-flux zone, separation was found to be very difficult and in some cases the lead was pulled from the fuel pellets with the cladding. However, the plates were originally filled with lead at a temperature of around 925°F, so the temperature alone does not explain the adhesion observed.

E. Fuel

No gross physical change in the fuel pellets due to irradiation was noted. The slight degree of cracking observed was uniform throughout both the in and out-of-pile plates (see Figures 12 and 13). This cracking was probably due to thermal shock and is not considered to detract from the overall serviceability of this type of fuel.

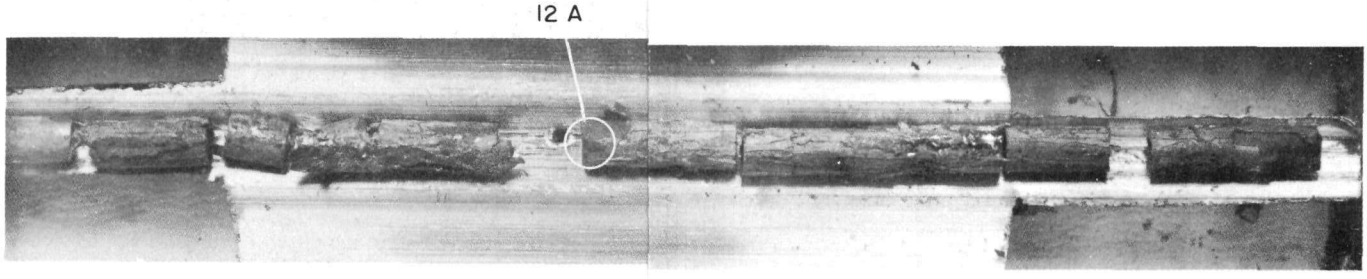
12 A

12 A

12 B

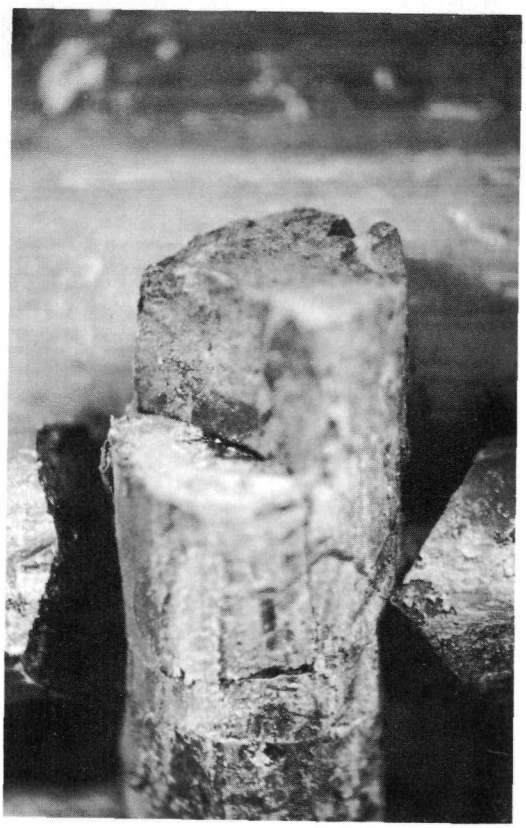

12 C

12 D

Figure 12

Fuel Pellets from In-pile Plate

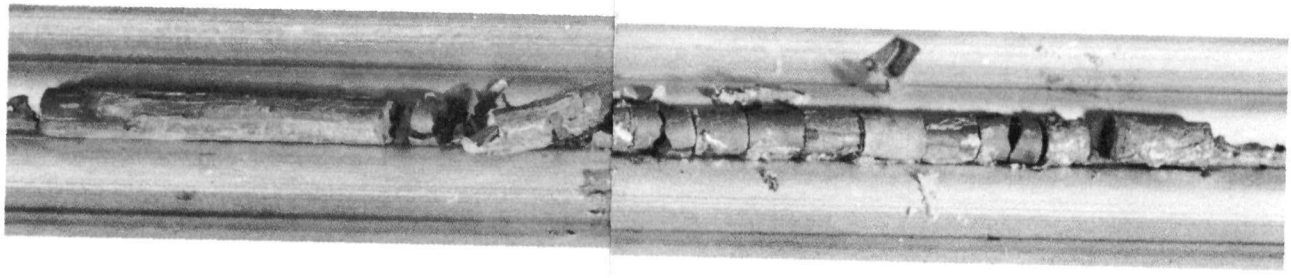

APPENDIX

Table 10

PHYSICAL DIMENSIONS OF PLATE #2 (IN-PILE)

NEW

Distance from In-reactor End (in.)	Width (in.)	Thickness, Top to Bottom (in.)			
		Channel Number			
		1	2	3	4
1	2.0016	0.3033	0.3034	0.3029	0.3033
2	2.0031	0.3034	0.3049	0.3039	0.3052
3	2.0034	0.3045	0.3053	0.3049	0.3057
4	2.0052	0.3051	0.3053	0.3068	0.3052
5	2.0060	0.3048	0.3055	0.3043	0.3052
6	2.0068	0.3047	0.3051	0.3046	0.3056
7	2.0056	0.3048	0.3046	0.3050	0.3060
8	2.0063	0.3054	0.3045	0.3050	0.3056
9	2.0057	0.3054	0.3050	0.3051	0.3055
10	2.0041	0.3055	0.3050	0.3052	0.3057
11	2.0045	0.3058	0.3054	0.3048	0.3057
12	2.0020	0.3060	0.3059	0.3058	0.3059
13	2.0038	0.3060	0.3064	0.3071	0.3065
14	2.0015	0.3063	0.3076	0.3070	0.3066
15	2.0000	0.3058	0.3077	0.3077	0.3070
16	1.8513				
Average	2.0040	0.3051	0.3054	0.3053	0.3057
Overall Length: Top - 16.076 in.; Center - 16.072 in.; Bottom - 16.064 in.					

Table 11

PHYSICAL DIMENSIONS OF PLATE #2 (IN-PILE)

AS REMOVED FROM REACTOR

Distance from In-reactor End (in.)	Width (in.)	Thickness, Top to Bottom (in.) Channel 3	Remarks
½	2.0019	0.3038	
1½	2.0077	0.3060	Loose red oxide over this area
2½	2.0141	0.3095	
3½	2.0092	0.3092	
4½	2.0050	0.3069	
5½	2.0049	0.3038	
6½	2.0042	0.3035	
7½	2.0040	0.3036	
8½	2.0010	0.3027	
9½	1.9991	0.3010	
10½	2.0005	0.3035	
11½	2.0001	0.3038	
12½	2.0007	0.3039	
13½	2.0005	0.3039	
14½	1.9978	0.3002	
15½	1.9909	0.1466	Fuel channel collapsed in this area
Average	2.0026		
Overall Length:[1] Top - 16.1230 in.; Center - 16.1196 in.; Bottom - 16.1010 in.			

[1] Length measurements on plate after removal from loop impaired due to damage to end of plate in removing from holding cartridge.

Table 12

PHYSICAL DIMENSIONS OF PLATE #2 (IN-PILE)

AFTER REMOVAL OF OXIDE

Distance from In-reactor End (in.)	Width (in.)	Thickness, Top to Bottom (in.)			
		Channel Number			
		1	2	3	4
1	1.9937	0.2960	0.2896	0.2958	0.2936
2	2.0068	0.2892	0.2970	0.2878	0.2913
3	2.0094	0.2963	0.3026	0.2987	0.3012
4	2.0052	0.3024	0.3038	0.3031	0.3020
5	2.0023	0.3020	0.3035	0.3018	0.2956
6	2.0023	0.3008	0.3023	0.3012	0.2995
7	2.0008	0.3016	0.3025	0.3012	0.2999
8	2.0011	0.3012	0.3022	0.3003	0.2999
9	1.9970	0.2993	0.3020	0.3003	0.2989
10	1.9969	0.3015	0.3016	0.2993	0.2990
11	1.9950	0.3006	0.3013	0.3001	0.2985
12	1.9971	0.3013	0.3022	0.2999	0.2998
13	1.9971	0.3016	0.3023	0.3023	0.3008
14	1.9982	0.3014	0.3029	0.3020	0.3013
15	1.9870	0.3008	0.2994	0.2979	0.3002
Average	1.999	0.2997	0.3010	0.2994	0.2988
Overall Length:[1] Top - 16.1232 in.; Center - 16.1056 in.; Bottom - 16.1125 in.					

[1] Length measurements on plate after removal from loop impaired due to damage to end of plate in removing from holding cartridge.

Table 13

PHYSICAL DIMENSIONS OF PLATE #4 (OUT-OF-PILE)

NEW

Distance from In-reactor End (in.)	Width (in.)	Thickness, Top to Bottom (in.)			
		Channel Number			
		1	2	3	4
1	1.9992	0.3024	0.2989	0.2988	0.3017
2	2.0003	0.3030	0.3012	0.2994	0.3021
3	2.0002	0.3032	0.3004	0.2990	0.3022
4	2.0009	0.3021	0.2998	0.2992	0.3016
5	2.0013	0.3018	0.3007	0.2985	0.3015
6	2.0014	0.3017	0.2999	0.2981	0.3012
7	2.0017	0.3017	0.2999	0.2980	0.3012
8	2.0018	0.3016	0.3001	0.2980	0.3009
9	2.0017	0.3016	0.3002	0.2980	0.3008
10	2.0022	0.3028	0.3001	0.2999	0.3018
11	2.0017	0.3027	0.3004	0.3004	0.3025
12	1.9999	0.3035	0.3011	0.3010	0.3032
13	1.9988	0.3040	0.3013	0.3012	0.3040
14	1.9997	0.3045	0.3018	0.3018	0.3055
15	1.9983	0.3060	0.2996	0.2997	0.3050
16					
Average	2.0006	0.3028	0.3004	0.2994	0.3024
Overall Length: Top - 16.075 in.; Center - 16.075 in.; Bottom - 16.076 in.					

Table 14

PHYSICAL DIMENSIONS OF PLATE #4 (OUT-OF-PILE)

AS REMOVED FROM REACTOR

Distance from In-reactor End (in.)	Width (in.)	Thickness, Top to Bottom (in.)			
		Channel Number			
		1	2	3	4
$\frac{1}{2}$	1.9976	0.2991	0.2930	0.2979	0.2967
$1\frac{1}{2}$	1.9987	0.3000	0.2957	0.2989	0.2992
$2\frac{1}{2}$	1.9986	0.3012	0.2976	0.2985	0.2989
$3\frac{1}{2}$	2.0047	0.3015	0.2965	0.2988	0.2985
$4\frac{1}{2}$	2.0038	0.2998	0.2966	0.2970	0.2982
$5\frac{1}{2}$	2.0020	0.3008	0.2962	0.2970	0.2988
$6\frac{1}{2}$	2.0001	0.3006	0.2971	0.2970	0.2991
$7\frac{1}{2}$	1.9999	0.3002	0.2983	0.2972	0.2988
$8\frac{1}{2}$	1.9991	0.2992	0.2995	0.2974	0.2985
$9\frac{1}{2}$	2.0032	0.2995	0.2992	0.2955	0.2985
$10\frac{1}{2}$	1.9971	0.3018	0.2999	0.2948	0.2982
$11\frac{1}{2}$	1.9993	0.3002	0.3005	0.2961	0.2997
$12\frac{1}{2}$	2.0008	0.3009	0.3007	0.2970	0.3001
$13\frac{1}{2}$	1.9975	0.3021	0.3005	0.2970	0.3001
$14\frac{1}{2}$	1.9895	0.3017	0.2998	0.2961	0.3000
$15\frac{1}{2}$	1.9815	0.1728[2]	0.1495[2]	0.1500[2]	0.1488[2]
Average[1]	2.0002	0.3006	0.2981	0.2971	0.2989
Overall Length: Top - 16.0717 in.; Middle - 16.0779 in.; Bottom - 16.0811 in.					

[1]Average does not include measurements of collapsed portion of tube.

[2]Measurement of collapsed tube.

Table 15

PHYSICAL DIMENSIONS OF PLATE #4 (OUT-OF-PILE)
AFTER REMOVAL OF OXIDE

Distance from In-reactor End (in.)	Width (in.)	Thickness, Top to Bottom (in.)			
		Channel Number			
		1	2	3	4
½	1.9943	0.2951	0.2918	0.2910	0.2930
1½	1.9938	0.2968	0.2928	0.2938	0.2961
2½	1.9949	0.2974	0.2941	0.2944	0.2952
3½	1.9943	0.2973	0.2935	0.2939	0.2948
4½	1.9954	0.2960	0.2933	0.2935	0.2947
5½	1.9949	0.2983	0.2933	0.2923	0.2961
6½	1.9968	0.2968	0.2948	0.2928	0.2959
7½	1.9959	0.2962	0.2950	0.2924	0.2955
8½	1.9974	0.2975	0.2952	0.2916	0.2948
9½	1.9953	0.2965	0.2955	0.2915	0.2945
10½	1.9939	0.2989	0.2968	0.2925	0.2933
11½	1.9953	0.2972	0.2969	0.2925	0.2952
12½	1.9944	0.2978	0.2969	0.2938	0.2964
13½	1.9932	0.2986	0.2956	0.2939	0.2974
14½	1.9861	0.2999	0.2976	0.2935	0.2960
15½	1.9796	0.1722[2]	0.1438[2]	0.1385[2]	0.1420[2]
Average[1]	1.9950	0.2974	0.2949	0.2929	0.2953
Overall Length: Top - 16.0770 in.; Middle - 16.0771 in.; Bottom - 16.0858 in.					

[1]Average does not include measurements of collapsed portion of tube.

[2]Measurement of collapsed tube.

REFERENCES

1. J. H. Handwerk and R. A. Noland, Oxide Fuel Elements for BORAX-IV, paper presented at the Technical Briefing Session held at Argonne National Laboratory, May 27-28, TID-7535, p. 140.

2. J. H. Handwerk and R. A. Noland, "Fabrication of Fuel Elements for the BORAX-IV Reactor," Progress in Nuclear Energy, Series V, Vol. 2, Metallurgy and Fuels, Pergamon Press.

3. J. E. Draley, C. R. Breden, W. Ruther and N. R. Grant, High-temperature Aqueous Corrosion of Aluminum Alloys, Proceedings of the Second United Nations International Conference on Peaceful Uses of Atomic Energy, Geneva, Switzerland (1958), Vol. 5, p. 113.

4. C. F. Reinke, Examination of BORAX-IV Defective Fuel Plates (to be published).

5. G. K. Whitham, W. R. Wallin and E. Graham, Locating Defective Fuel Elements in BORAX-IV, paper presented at the American Nuclear Society Meeting, Gatlinburg, Tennessee, June 15-17, 1959.

6. G. Ervin Jr. and E. F. Osborn, The System Al_2O_3-H_2O, Journal of Geology, 59, 381 (1951).

7. E. L. Martinec, Pressurized-water Test Loop at MTR, Nucleonics, 15 (4), 73 (1957).

8. C. R. Breden, I. Charak and R. H. Leyse, Summary of Investigations on Deposits and Scale in EBWR, ANL-6136 (to be published).

9. G. V. Bicfer and P. G. Anderson, Corrosion Behavior of Aluminum-Nickel-Iron Alloys in High-temperature Water Under Dynamic Conditions, CR Met-799

ACKNOWLEDGEMENT

The author wishes to acknowledge the assistance of the following persons who aided in the various phases of this experiment.

N. R. Grant	ANL Reactor Engineering Div.	Set up of experiment and original calculations. Advice on aluminum corrosion and stripping technique.
E. L. Martinec	ANL Reactor Engineering Div.	Original calculations.
C. C. Crothers	ANL Representative at MTR	Operation of experimental loop during irradiation.
J. H. Handwerk and R. A. Noland	ANL Metallurgy Div.	Manufacture of test plates.